第51卷第4期 中国科学技术大学学报 Vol. 51, No. 4
2021年4月 JOURNAL OF UNIVERSITY OF SCIENCE AND TECHNOLOGY OF CHINA Apr. 2021
Received: 2021-01-07; Revised: 2021-02-21 doi:10.52396/JUST-2020-0018

The performance analysis on a novel purified PV-Trombe wall for electricity, space heating, formaldehyde degradation and bacteria in activation

LI Niansi[1,2], LIU Xiaoyong[2,3], YU Bendong[1*]
1. Department of Thermal Science and Energy Engineering, University of Science and Technology of China, Hefei 230026, China
2. Inspection and Testing Center, Hefei Institute for Public Safety Research, Tsinghua University, Hefei 230601, China
3. Anhui Province Key Laboratory of Human Safety, Hefei, 230602, China
* Corresponding author. E-mail: bendong@mail.ustc.edu.cn

Abstract: On the one hand, PV-Trombe wall is a combined solar system that meets dual functions of space heating and electricity output, but the utilization on the recovered solar heat by PV-Trombe wall is very limited. On the other hand, thermal catalytic oxidation and thermal sterilization are two advanced air purification technologies and both they have huge application potential with solar heat. Therefore, a novel purified PV-Trombe wall for electricity, space heating, formaldehyde degradation and bacteria inactivation was proposed. Firstly, the system thermal and mass transfer model was established and verified by experimental data. Secondly, the comprehensive performance with the PV coverage ratio of 0 was analyzed. Finally, the effect of PV coverage ratio on the system performance was investigated. Accordingly, the main results were: ① Under PV coverage ratio of 0, the average daily air thermal efficiency and formaldehyde single-pass ratio were 0.46 and 0.35, respectively. Meanwhile, the total generated volume of clean air by formaldehyde degradation was 93.4 m^3. Five kinds of bacteria were fully thermal inactivated for several hours. Accordingly, the total generated volume of clean air were 188.3, 173.0, 201.4, 189.9 and 200.2 m^3 for E. coli, L. monocytogenes, L. plantarum, S. Senftenberg and S. cerevisiae, respectively. ② The PV coverage ratio played a different role on the system comprehensive performances. For specific performances, the PV coverage ratio only had a positive influence on electrical performance and had negative effect on other performances such as thermal, formaldehyde degradation and bacteria inactivation performances. However, considering the system comprehensive performances, the electrical energy was the additional product and the low PV coverage ratio was suggested. ③ The works could provide possible support to the prevention and control of COVID-19.

Keywords: Trombe wall; PV; solar thermal sterilization; solar thermal catalytic oxidation; space heating
CLC number: TU832.5 **Document code**: A

1 Introduction

Trombe wall has been investigated for a long time due to its several advantages such as the simple structure, low maintenance cost and stable property since two French architects Felix Trombe and Jacques Michel designed it in 1967[1]. However, Trombe wall still has the disadvantages of the single-function, low energy efficiency and overheating.

To improve the status of Trombe wall, many researchers have conducted a lot of works on the modifications and improvements. Rabani et al[2] proposed a novel designed Trombe wall that could receive the solar radiation from three different directions. The experimental results showed that the indoor air temperature had an increase of 3 ~ 6 ℃ compared with conventional Trombe wall. Zhou et al[3] proposed a composite Trombe wall with a water wall and found that the thermal efficiency was 7.2% higher than the conventional Trombe wall. Ma et al[4] added the designed pipes with the fan in Trombe wall and the thermo-circulation could be controlled. The results showed that the proposed wall could reduce the annual energy cost up to 3.7% with the optimized ventilation.

Citation: LI Niansi, LIU Xiaoyong, YU Bendong. The performance analysis on a novel purified PV-Trombe wall for electricity, space heating, formaldehyde degradation and bacteria inactivation. J. Univ. Sci. Tech. China, 2021, 51(4): 308-318.

Hong et al[5] applied a novel venetian blind in a conventional Trombe wall. The venetian blind consisted of a high absorptive layer and a high reflective layer on each side. The venetian blind could absorb and reflect the solar heat in winter and summer, respectively. Rabani et al[6] proposed a Trombe wall combined with solar chimney and water spraying system and conducted an experimental study. The results showed that the water spraying system decreased the indoor temperature by 8 ℃ and increased the indoor relative humidity by 17%, respectively.

In summary, the above works on the Trombe wall are all aimed to improve the thermal performance such as heating efficiency and thermal comfort. To increase the energy quality, a PV-Trombe wall system that combined Trombe wall with PV modules was proposed. Ji et al[7, 8] firstly laminated PV cells on the glazing cover of conventional Trombe wall and the combined wall was greatly improved in the comprehensive performance because the energy level of electrical energy was greatly higher than thermal energy. The experimental results showed that average electrical efficiency could reach 10% ~ 11% and a temperature increase of indoor air temperature with a maximum value of 14.42 ℃ was approached compared with the referenced system[7]. Afterwards, a novel PV Trombe wall was proposed by Ji et al[9] that the PV panel was located in the middle of air flow channel. They found that the thermal efficiency had a certain degree of increase while no influence on the electrical efficiency. In addition, considering the overheating problem in summer, Ji et al[10, 11] proposed a multifunctional PV-Trombe wall that performed the functions of electrical generation in whole year, space heating in winter, and hot water production in summer.

In addition, the indoor air quality (IAQ) has been paid more and more focus by people due to the indoor release by volatile organic compounds (VOCs). Meanwhile, the bacteria and viruses will breed and grow inside the air-conditioning systems quickly due to the dark and damp environment[12]. The bioaerosol formed by theses bacteria and viruses flows into the indoor environment and then causes human diseases[13]. The current Corona Virus Disease 2019 (COVID-19) has brought great disasters and losses to people in the world. What should not be ignored is especially in winter, the tight rooms provide the conditions for the accumulation and spread of gaseous pollutants and the bioaerosol.

The indoor VOCs removal technologies such as adsorption[14], thermal catalytic oxidation (TCO)[15] and photocatalytic oxidation (PCO)[16] have been widely reported. However, for the adsorption purification technology, the problems of difficult regeneration, easy saturation and secondary pollution have been reported[17]. The main barrier for photocatalytic purification technology is that the band gap of photocatalyst TiO_2 greatly determine the utilization on solar energy. The light response range is only Ultraviolet (UV) light and the ratio in solar spectra is only 5%. Thermal catalytic oxidation purification is an advanced air cleaning method and has several advantages such as high removal efficiency, simple equipment, and no secondary pollution[18]. Thermal catalytic oxidation process is realized through the catalytic oxidation reaction between the thermal catalysts and the gaseous pollutant under the thermal effect[19]. Apparently, the thermal energy used for driving the thermal catalytic oxidation can come from the solar systems easily.

For the control strategies on the bioaerosol, several methods have been proposed. UV radiation has a germicidal effect, thus several studies were conducted to investigate the effect of UV irradiation on the viability of the bioaerosol[20]. However, the UV light has harmful effect on the human skin. The electric ion emission method was also investigated as a mean of controlling the bioaerosol[21]. While, it exists some shortcomings such as the generation of ozones and the electric charge accumulation on surrounding surfaces. The thermal inactivation has long been considered as a most suitable method to control the bioaerosol[13]. The environment of 45 ℃ could inhibit the self-repair of DNA and RNA of the bacteria and viruses[22]. Furthermore, the environmental temperature was above 55℃, the DNA and RNA of bacteria and viruses would be destroyed[23]. For the solar application systems, the air could be heated up to 50 ~ 80 ℃[24], which could provide the feasibility for the application of thermal sterilization technology in solar systems.

Therefore, in this article, we have combined thermal catalytic oxidation and thermal sterilization with PV-Trombe wall, and proposed a novel purified PV-Trombe wall for electricity, space heating, formaldehyde degradation and bacteria inactivation. Firstly, we proposed a novel purified PV-Trombe wall; Secondly, the system thermal and mass transfer model was established; Thirdly, the comprehensive performance with the PV coverage of 0 was analyzed; Finally, the effect of the PV coverage on the system performance was investigated.

2 System descriptions

Figure 1 shows the schematic diagram of the novel purified PV-Trombe wall. From the outdoor to the indoor, in turn, the combined Trombe wall consists of the glazing cover, the closed air layer, the PV panel, the absorber plate, the air flow channel, the back plate,

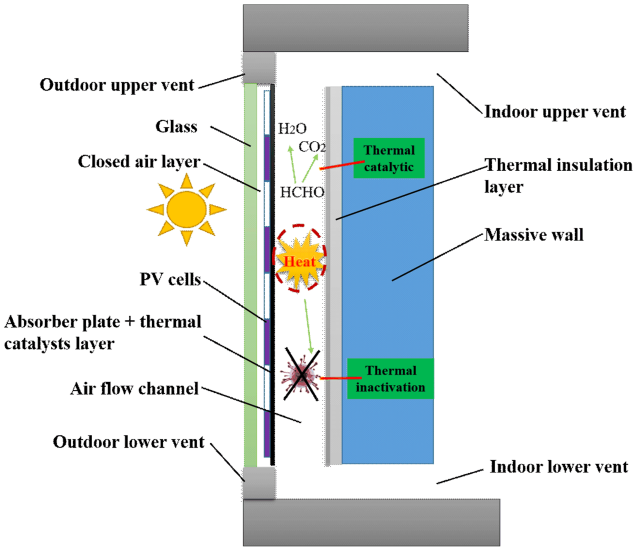

Figure 1. The schematic diagram of a novel purified PV-Trombe wall.

the thermal insulation materials, the massive wall and four vents. The compound transition metal oxides MnO_x-CeO_2 are used as the thermal catalysts[25]. Under solar radiation, both the indoor upper and lower vents are opened, the outdoor upper and lower vents are closed. The solar rays illustrate the PV panel, a part of solar radiation is converted in to the electrical energy. The rest solar radiation is converted into the thermal energy and the temperature of the absorber plate with PV cells is increased. At the same time, the thermal catalysts are heated and the temperature is increased. The air in the air flow channel is heated by the thermal catalyst layer and begins to flow under the thermos-syphon effect. The formaldehyde is removed by the thermal catalytic oxidation reaction over the thermal catalysts when the light-off catalytic temperature is approached. Meanwhile, the bacteria and virus dispersed in the air flow are inactivated under the heat effect when the air and residence time in the air flow channel approach a certain level.

3 Experimental, models and performance evaluation

The system performance including the electrical performance, the thermal performance, the performances of formaldehyde removal and the thermal inactivation of bacteria were investigated. The Trombe wall systems were installed as a south wall of a building in Xining City, Qinghai Province. The thermal performance was investigated based on the experimental tests. While, limited to experimental conditions, the electrical performance and the purification performance were investigated by the numerical method.

Figure 2. The experimental photos of the purified Trombe wall in Qinghai.

3.1 Experimental

A field experiment was carried out to investigate the system thermal performance, which was shown in Figure 2. The sizes of testing room are 6000 mm (length) * 3000 mm (width) * 3000 mm (height). The sizes of the hybrid Trombe wall are 1000 mm (length) * 2000 mm (height). The area of both the upper vent and lower vent are 0.048 m^2.

The needed measuring parameters included the solar radiation intensity, the ambient temperature, the ambient wind velocity, the air flow velocity in the air flow channel, and various layer temperatures of Trombe wall system. The meteorological parameters including the solar radiation intensity and the ambient temperature were recorded by the local meteorological station. The various layer temperatures including the glass cover, the absorber plate, the back plate, the massive wall, the air at inlet outlet, and the indoor air were tested by copper-constantan thermocouple, with the accuracy of ±0.5 ℃. The air flow velocity in the air flow channel was measured by a hot-wire anemometer (KANOMAX), with the accuracy of ±0.01 m · s^{-1}. The experiment was conducted on 19th October, 2015. The indoor upper vent and lower vent were opened from 9:00 to 18:00 and closed at the other time. The temperature and solar radiation intensity data were recorded with an interval of 30 s. Hot-wire anemometer measured the air velocity in the cavity every 10 min. The experimental environmental data were shown in Figure 3. The average ambient temperature and global solar radiation intensity were 18.1 ℃ and 620.6 W · m^{-2}, respectively.

3.2 System model

For the glazing cover, the heat transfer can be dealt with a node:

$$c_g m_g \frac{\partial T_g}{\partial t} = \alpha_g I + h_{c,e}(T_e - T_g) + h_{r,e}(T_{\text{sky}} - T_g) + (h_{r,p,g} + h_{c,a})(T_{ap} - T_g) \quad (1)$$

where, T_g, T_e, T_{sky} and T_{ap} are respectively the temperature of the glazing cover, ambient, sky and absorber plate with PV cells, ℃. I is the solar radiation

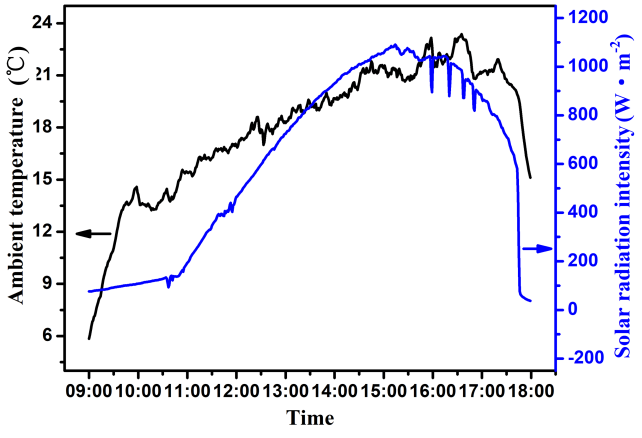

Figure 3. The experimental environmental data including solar radiation intensity and ambient air temperature.

intensity, W · m^{-2}. $h_{r,p,g}$ is the radiative heat transfer coefficient between the glazing cover and the absorber plate with PV cells, which has the following equation[26]:

$$h_{r,p,g} = \sigma(T_g^2 + T_{ap}^2)(T_g + T_{ap}) \frac{\xi}{1/\varepsilon_{PV} + \xi(1/\varepsilon_g - 1)} + \frac{1-\xi}{1/\varepsilon_{black} + (1-\xi)(1/\varepsilon_g - 1)} \quad (2)$$

where ξ is the PV coverage ratio of the PV module.

As for the absorber plate with PV cells, the one-dimensional thermal transfer model is expressed as follows:

$$c_p m_p \frac{\partial T_{ap}}{\partial t} = \lambda_p \delta_p \left(\frac{\partial^2 T_{ap}}{\partial x^2} + \frac{\partial^2 T_{ap}}{\partial z^2}\right) + h_{c,p,a}(T_a - T_{ap}) + (h_{r,a} + h_{c,a})(T_g - T_{ap}) + h_{r,p,b}(T_b - T_{ap}) + I\tau_g\alpha_{ap} - \xi E_{PV} \quad (3)$$

where, T_a and T_b are the temperature of the air flow in the air flow channel and the back plate, respectively, ℃. $h_{c,p,a}$ is the convective heat transfer coefficient between of the absorber plate with the air in the air flow channel, W · m^{-2} · K^{-1}. The calculation of $h_{c,p,a}$ can be referred to the following empirical equation under natural convection conditions[27]:

$$Nu = 0.12(GrPr)^{1/3} \quad (4)$$

$$h_{c,a,p} = \frac{\lambda_a Nu}{\delta_a} \quad (5)$$

E_{PV} is the PV output electrical power, which has the following equation:

$$E_{PV} = I\tau_g\xi\eta_{ref}[1 - B_r(T_{PV} - T_{ref})] \quad (6)$$

where, η_{ref} is the standard efficiency of the polysilicon silicon PV cell with the value of 0.203 under referenced conditions[28]. B_r is the cell temperature coefficient referred to the value of 0.0045 K^{-1}[6, 43].

The air flow in the air flow channel has three

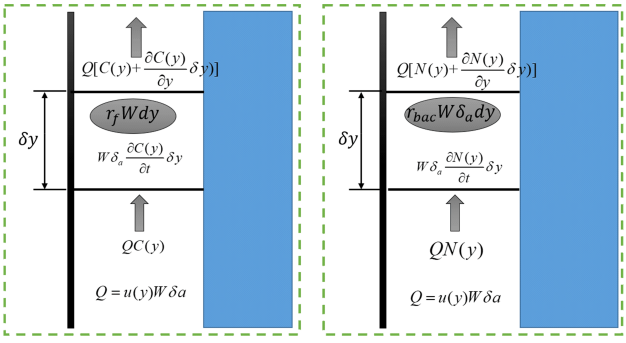

Figure 4. The schematic presentation of the mass transfer micro unit of the purified PV-Trombe wall.

processes including the thermal transfer process, the thermal-catalytic process and the thermal inactivation process, of which the heat and mass transfer in a micro unit, which was shown in Figure 4. Two assumptions were made: ① The reaction heat generated by a thermal catalytic oxidation reaction was ignored because of the low concentration of the indoor formaldehyde concentration[19]; ② The bacteria transport loss in the air flow channel was ignored[13]. The heat and mass transfer models were considered as the one-dimensional model. The thermal and mass transfer models are expressed as follows:

$$\left.\begin{aligned} c_a m_a \frac{\partial T_a}{\partial t} &= h_{c,p,a}(T_{ap} - T_a) + h_{c,b,a}(T_b - T_a) - \rho_a u\delta_a c_a \frac{\partial T_a}{\partial y} \\ \frac{\partial C}{\partial t} + u\frac{\partial C}{\partial y} + \frac{r_f}{\delta_a} &= 0 \\ \frac{\partial F}{\partial t} + u\frac{\partial F}{\partial y} + r_b &= 0 \end{aligned}\right\} \quad (7)$$

where, C (ppb) and F (CFU · m^{-3}) are the formaldehyde concentration and the bacteria concentration of the air mainstream in the air flow channel, respectively. u is the air flow velocity in the air flow channel, m · s^{-1}, which can be calculated by the following equation under natural flow conditions:

$$u = \sqrt{\frac{2g\beta(T_{a\_out} - T_{a\_in})H}{C_1(A/A_v)^2 + C_2}} \quad (8)$$

where C_1 and C_2 are the constants related to the channel structure and size.

r_f(ppb · m · s^{-1}) and r_b(CFU · m^{-3} · s^{-1}) are the formaldehyde removal rate and the thermal inactivation rate of bacteria. According to Reference [29], as for the thermal catalytic oxidation process, a mass conservation under the steady state is existed on the air-catalysts interface, which can be expressed as follows:

$$r_f(z) = k_{app}(z)C_s(z) = m(z) = h_m(z)(C(z) - C_s(z)) \quad (9)$$

where k_{app} is the apparent reaction coefficient, $m \cdot s^{-1}$; C_s is the surface formaldehyde concentration near to the catalysts layer, ppb; m is the formaldehyde mass transfer rate from the air flow to the catalysts layer; h_m is the formaldehyde mass transfer coefficient at the catalysts surface, $m \cdot s^{-1}$, which can be obtained by Chiltong-Colburn analogy[30]. According to Equation (9), C_s can be calculated by the following equation:

$$C_s(z) = \frac{C(z)}{1 + k_{app}(z)/h_m(z)} \tag{10}$$

In our previous studies, we have deduced the reaction kinetic of thermal catalytic oxidation of formaldehyde in theory, which was verified by the experimental data[15]. The thermal catalytic reaction rate r_f is closely related to the catalytic temperature and surface concentration.

$$r_f = \frac{kK e^{-\frac{E}{RT}} e^{-\frac{H}{RT}} C_s}{(1 + K e^{-\frac{H}{RT}} C_s)^2} \tag{11}$$

According to the definition, the thermal inactivation rate of bacteria in Equation (7), r_b, is the value of the total differential of $N(T, t)$ to the time, which is equal to the partial differential of N to t because the air temperature at the micro unit shown in Figure 3 can be assumed as the constant. Then the expression is

$$r_b = -\frac{dN}{dt} \tag{12}$$

where, the expression of N refers to the Gauss-Eyring model, which is generally used for describing the thermal inactivation performance of bacteria under different temperature and residence time[32].

$$\log_{10}\left(\frac{n(t,T)}{N_0}\right) = \log_{10}\left(\frac{1}{2}\mathrm{erfc}\left(\frac{T - T_c(t)}{\sigma\sqrt{2}}\right)\right) \tag{13}$$

where $N(t, T)$ is the surviving bacteria number under the conditions of temperature T residence time t, N_0 is the initial bacteria number, T_c is the critical temperature, which represents the transition temperature that the bacteria begins to be inactivated. T_c is a function of the residence time t and the characteristic temperature Z, which is calculated by the following equation:

$$T_c(t) = T_r - Z\log_{10}\left(\frac{t}{\tau}\right) \tag{14}$$

where τ is chosen as 1 s and T_r is the reference temperature[32].

According to Reference [33], the fitting parameters of the thermal inactivation of five different bacteria using the Gauss-Eyring model were presented in Table 1.

Table 1. The fitting parameters of the thermal inactivation of five different bacteria using the Gauss-Eyring model[33].

Bacteria types	σ	T_r(℃)	Z	R^2
E. coli	1.32	64.5	5.8	0.86
L. monocytogenes	1.38	70.8	7.6	0.65
L. plantarum	1.29	58.8	4.5	0.65
S. Senftenberg	1.49	64.2	6.9	0.74
S. cerevisiae	1.36	59.1	3.3	0.85

For back plate, the thermal transfer is assumed to a one-dimensional model:

$$c_b m_b \frac{\partial T_b}{\partial t} = \lambda_b \delta_b \frac{\partial^2 T_b}{\partial z^2} + h_{c,a,b}(T_a - T_b) + h_{r,p,b}(T_{ap} - T_b) + \frac{T_{w\_i=1} - T_b}{R_{b,w}} \tag{15}$$

For massive wall,

$$c_w m_w \frac{\partial T_w}{\partial t} - \lambda_w \frac{\partial^2 T_w}{\partial y^2} = 0 \tag{16}$$

3.3 Performance evaluation index

The high-performance purified PV-Trombe wall has multiple functions integrated in one unit such as electrical generation, space heating, air purification and inactivation of bacteria. To comprehensively evaluate the system performance, the air heating efficiency, the electrical efficiency, the formaldehyde removal efficiency and bacteria inactivation efficiency were applied.

The instantaneous air heating and electrical efficiencies are respectively expressed as follows:

$$\eta_t = \frac{c_a m(T_{a\_out} - T_{a\_in})}{IA} \tag{17}$$

$$\eta_e = \frac{E_{pv}}{IA} \tag{18}$$

Accordingly, the daily thermal and electrical efficiencies are the integral calculations of Equations (17) and (18) to the time, respectively.

As for the formaldehyde removal efficiency and bacteria inactivation efficiency, the single-pass conversion ratio and the clean air delivery rate (CADR) are used for the evaluations. CADR is defined as the volume of fresh air generated per hour.

$$\varepsilon = \frac{X_{in} - X_{out}}{X_{in}} \tag{19}$$

$$\mathrm{CADR} = Q\varepsilon \tag{20}$$

Accordingly, the total generated volume of clean air is calculated by the integral calculation of CADR to the time.

4 Results and discussions

Figure 5 shows the comparison between the predicated

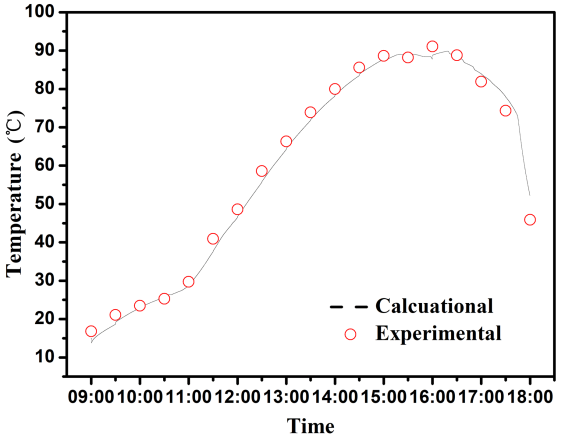

Figure 5. The verification on the outlet air temperature.

and experimental outlet air temperature, which can provide enough accuracy of the thermal model. While, limited to experimental conditions, the electrical performance, the performances of formaldehyde degradation and thermal inactivation of bacteria were investigated by the numerical method. The verifications on the electrical model and formaldehyde degradation models can be referred to in our previous studies[15, 31, 34]. The data of outlet formaldehyde concentration were referred to the previous experimental investigations on the thermal-catalytic-Trombe wall system[31]. The data of output electrical power were referred to in the previous experimental investigations on the PV-Trombe wall system[9]. By calculations, the RMSDs (root mean square deviations) of the outlet air temperature, outlet formaldehyde concentration and output electrical power are 1.2%, 5.8% and 4.2%, respectively. As for the simulations of thermal inactivation of bacteria, the simulation results are not groundless since the simulation was based on the experimental results of Reference [33]. In summary, the models have enough accuracy on the predictions on the system comprehensive performance in the following parts. Thus, the following discussions are all based on the numerical method.

4.1 The performance with PV coverage ratio of 0

Figure 6 shows the air thermal efficiency versus the time when the PV coverage is 0. From the curve, the instantaneous thermal efficiency was in the range of 0.1 ~ 0.6. Accordingly, by calculation, the average daily air thermal efficiency was 0.46. Figure 7 shows the outlet formaldehyde concentration, the formaldehyde single-pass conversion ratio and CADR versus the time

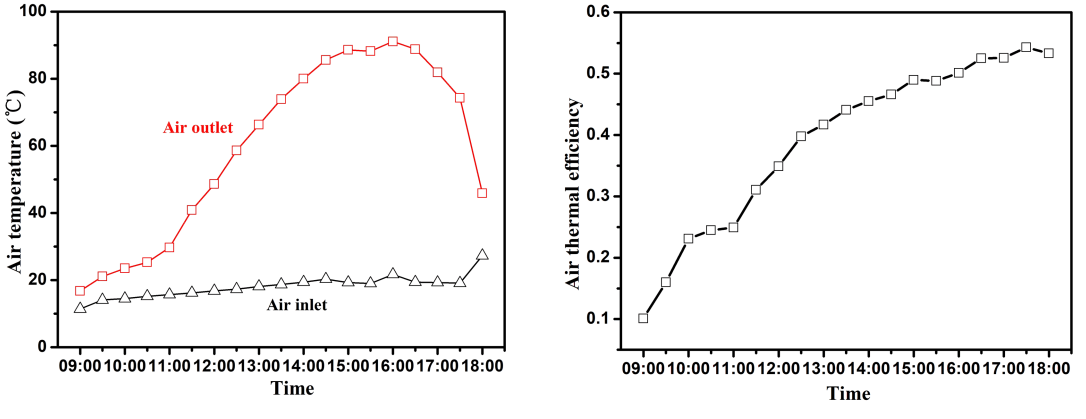

Figure 6. The air thermal efficiency with the PV coverage ratio of 0.

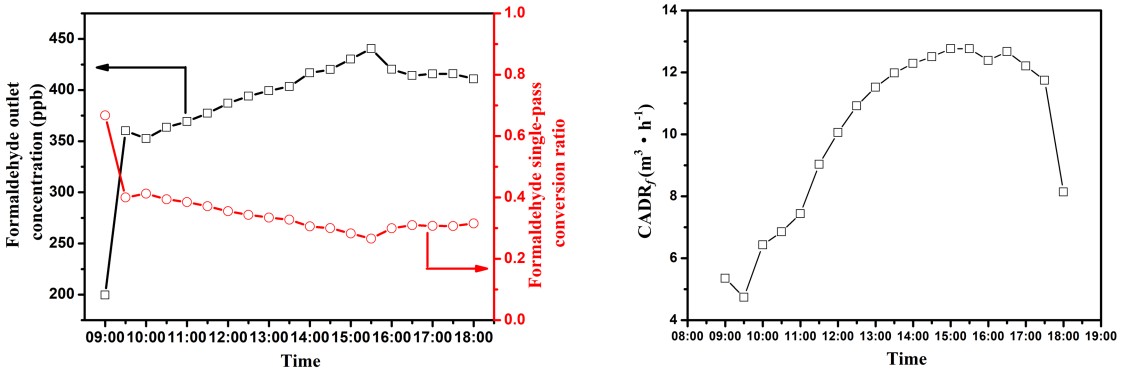

Figure 7. The outlet formaldehyde concentration, the formaldehyde single-pass conversion ratio and CADR versus the time with the PV coverage ratio of 0 with the formaldehyde inlet concentration of 600 ppb.

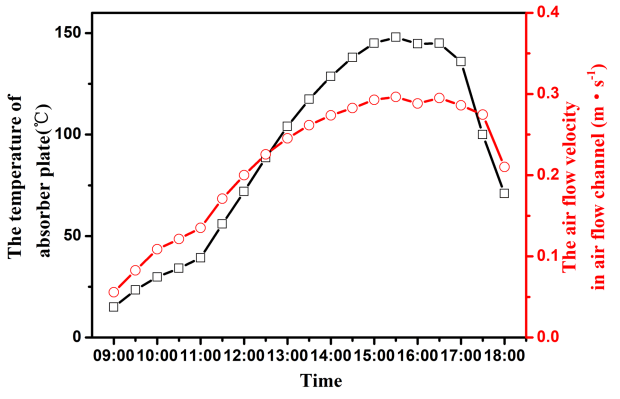

Figure 8. The air flow velocity in air flow channel and the temperature of absorber plate.

when the PV coverage is 0. Based on the previous studies, the formaldehyde single-pass conversion ratio decreased with the air volume flow rate and increased with the thermal catalytic temperature[25, 29, 35]. Based on experiments, the thermal catalysts approached relative high temperature levels (>80℃, Figure 8) and the effect of the thermal catalytic temperature on the formaldehyde single-pass conversion ratio was very limited. At the beginning, both the air volume flow rate in air flow channel and the thermal catalytic temperature increased (Figure 8). Although the increased thermal catalytic temperature enhanced the thermal catalytic performance, the increased air volume flow rate decreased the thermal catalytic performance by a large degree. Therefore, the single-pass conversion decreased with the time. Then the formaldehyde single-pass conversion ratio approached the minimum value at around 15:30 PM. At last, as the decrease of the solar radiation intensity, the formaldehyde single-pass ratio gradually increased because of the decrease of air volume flow rate in air flow channel although the decrease of the catalyst temperature (Fig. 8).

From the curves, the outlet formaldehyde concentration and formaldehyde single-pass conversion ratio were in the range of 200 ~ 450 ppb and 0.2 ~ 0.7, respectively. It is worth noting that the indoor gaseous formaldehyde will be fully degraded after the several times circular degradation although the single-pass conversion ratio is not 100%. The CADR was in the range of 4 ~ 14 $m^3 \cdot h^{-1}$ under the investigative conditions. The total generated clean air without gaseous formaldehyde was 93.4 m^3 by calculation.

The thermal inactivation performance of five kinds of bacteria including E. coli, L. monocytogenes, L. plantarum, S. Senftenberg and S. cerevisiae under the investigative conditions were calculated by the established heat and mass transfer models when the PV coverage was 0. Figure 9 shows the plots of the single inactivation ratio and CADR of five kinds of bacteria versus the time. From the curves, five kinds of bacteria began to be inactivated after about 12:00 because the sterilization temperature level was reached at this temperature point. Before 12:00, the outlet concentrations of all bacteria were the inlet concentrations of 3000 CFU · m^{-3} and all the single inactivation ratios were 0 all the time. Then, with the increase of solar radiation intensity, the air temperature in air flow channel increased quickly. Accordingly, the outlet concentrations of five kinds of bacteria decreased and the single inactivation ratio increased to 1 quickly. After about 17:00, the outlet concentrations gradually approached to 3000 CFU · m^{-3} and the single inactivation ratio decreased to 0 because the air temperature decreased quickly. Different kind of bacteria has different thermal inactivation performances under the same thermal conditions. Thus, the resistance on thermal process for five kinds of bacteria follows the order of L. monocytogenes < E. coli < S. Senftenberg < L. plantarum < S. cerevisiae. Accordingly, the values of CADR for five kinds of bacteria were in the range of 0 ~ 40 $m^3 \cdot h^{-1}$. The total generated clean air for E.

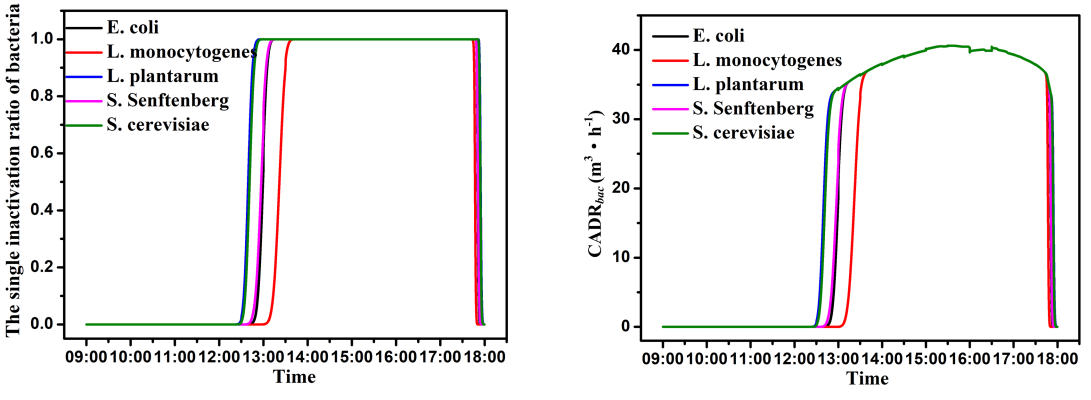

Figure 9. The single inactivation ratio and CADR of five kinds of bacteria including E. coli, L. monocytogenes, L. plantarum, S. Senftenberg and S. cerevisiae with all the inlet concentration of 3000 CFU · m^{-3}.

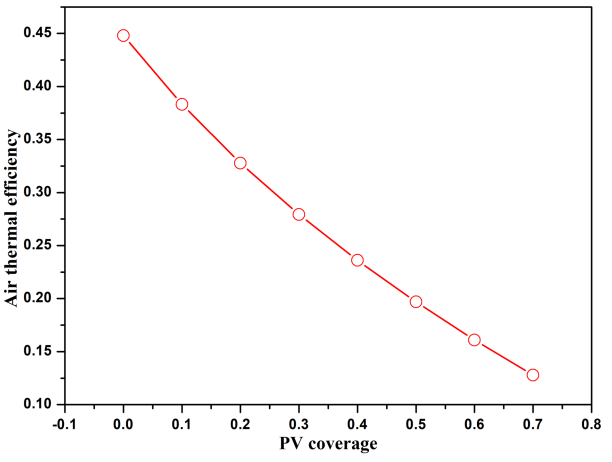

Figure 10. The average air thermal efficiency under different PV coverages.

coli, L. monocytogenes, L. plantarum, S. Senftenberg and S. cerevisiae were 188.3, 173.0, 201.4, 189.9 and 200.2 m^3, respectively.

4.2 The performance with different PV coverages

The PV coverage plays an important role on the system comprehensive performance. Therefore, the effect of PV coverage on the system performance were investigated in this part.

Figure 10 shows the average air thermal efficiency under different PV coverages. With the increase of PV coverage, the average air thermal efficiency decreased from 0.45 to 0.12 when the PV coverage increased from 0 to 0.7. With the increase of PV coverage, more solar energy was converted to electrical energy and obtained solar heat by air in the air flow channel. The curves of the instantaneous electrical efficiency and average electrical efficiency under different PV coverages were shown in Figure 11. The instantaneous electrical efficiency presented a downward parabola-type trend versus the time. At the beginning, with the increase of solar radiation intensity, the cell temperature increased quickly and then the electrical efficiency decreased. The electrical efficiency approached the minimum value at around 15:30. Afterwards, with the decrease of solar radiation intensity, the cell temperature decreased and the electrical efficiency increased gradually. From Figure 11, the average electrical efficiency decreased from 0.127 to 0.172 when the PV coverage increased from 0.1 to 0.7.

Figure 12 shows the formaldehyde single-pass ratio and CADR under different PV coverages. The formaldehyde single-pass ratio increased with the increase of the PV coverage. On the one hand, with the increase of solar radiation intensity, the temperature of thermal catalytic layer increased. The formaldehyde single-pass ratio increased with the temperature of thermal catalytic layer. As for the case with bigger PV coverage, the formaldehyde single-pass ratio presented less values. On the other hand, with the increase of solar radiation intensity, the air temperature in air flow channel increased and the air temperature difference between the air inlet and air outlet increased accordingly. The air mass flow rate increased with the increased air temperature difference between the air inlet and air outlet. For the setting constant inlet formaldehyde concentration, the needed degraded mass of formaldehyde increased with the air mass flow rate. The air mass flow rate played bigger effect on the formaldehyde single-pass ratio compared with a thermal catalytic temperature. The value of CADR decreased with the increase of the PV coverage. The maximum CADR was 12.5, 12.1, 11.3, 10.5 and 9.6 $m^3 \cdot h^{-1}$ when the PV coverage was 0, 0.1, 0.3, 0.5 and 0.7, respectively. The total generated fresh air decreased from 91.5 m^3 to 66.6 m^3 when the PV coverage increased from 0 to 0.7.

Figure 13 shows the single-pass inactivation ratio and CADR of E. coli and L. monocytogenes versus the time under different PV coverages. From the curves, we could see that the PV coverage played a decisive role on

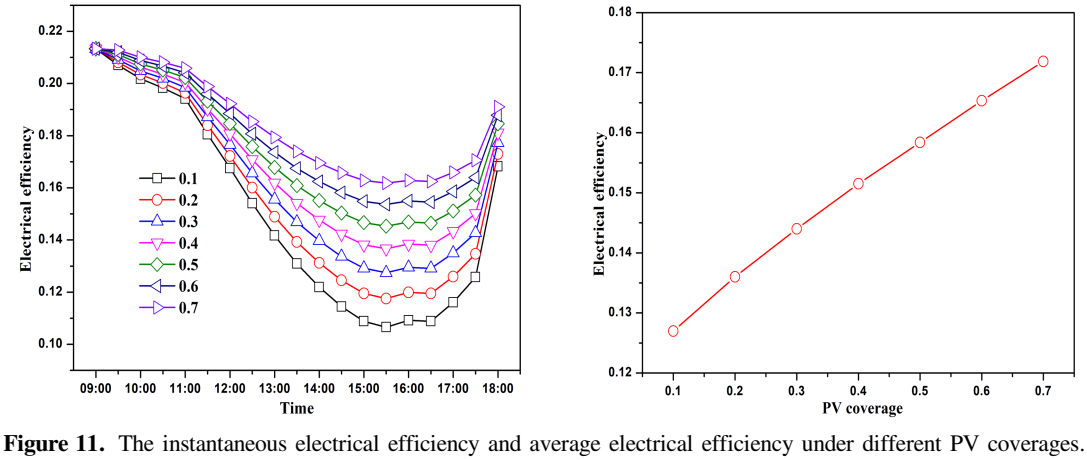

Figure 11. The instantaneous electrical efficiency and average electrical efficiency under different PV coverages.

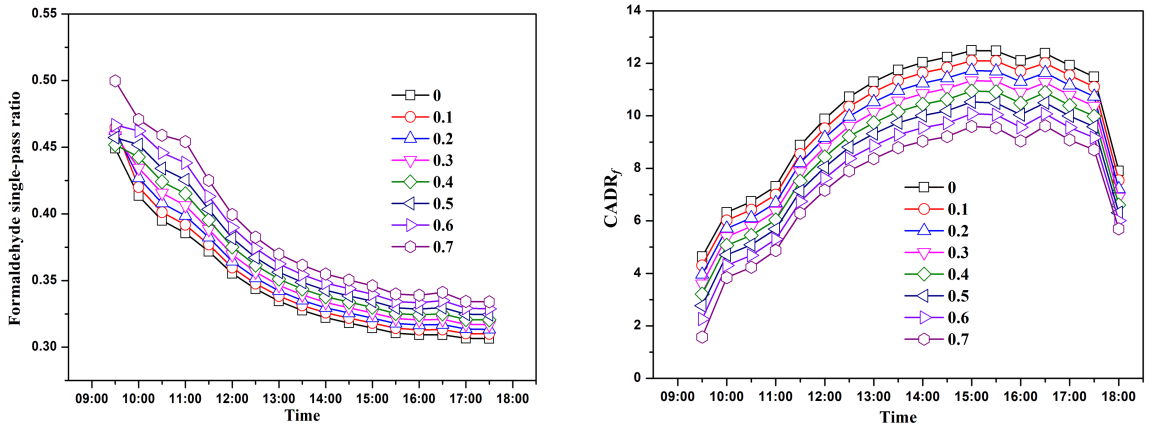

Figure 12. The formaldehyde single-pass ratio and CADR under different PV coverages with the inlet concentration of 600 ppb.

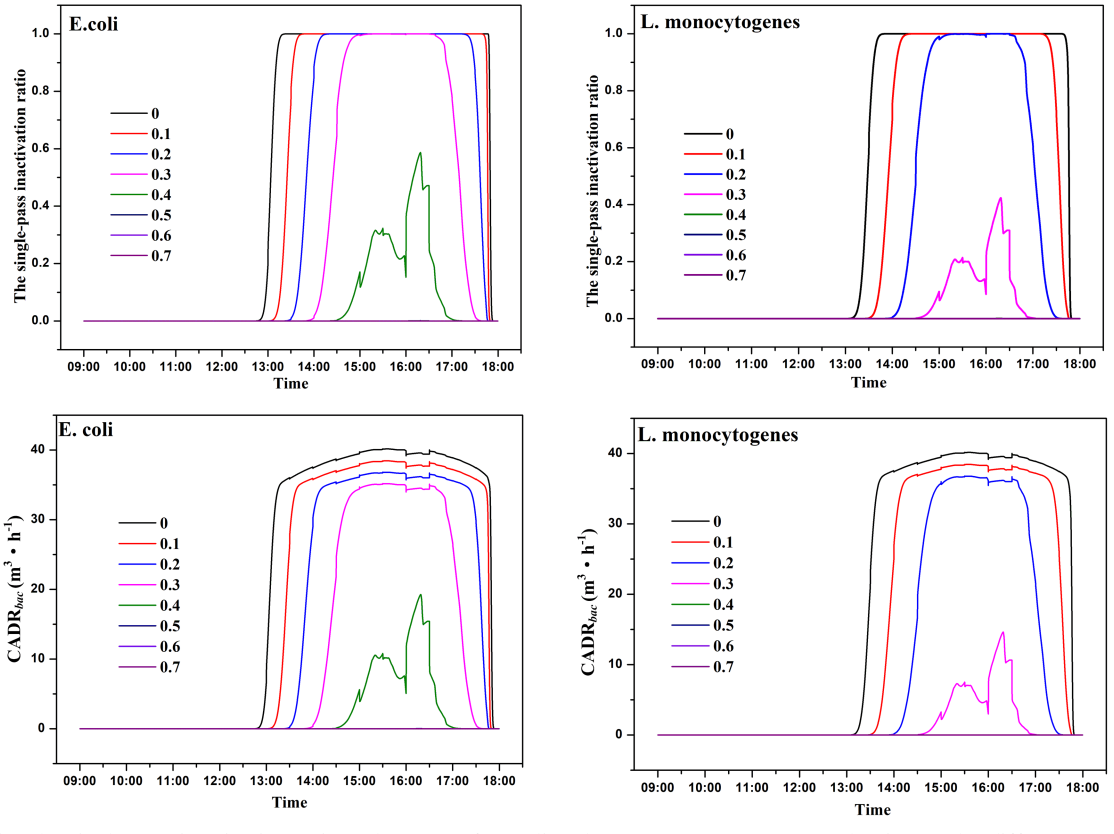

Figure 13. The single-pass inactivation ratio and CADR of E. coli and L. monocytogenes versus the time under different PV coverages with the inlet concentration of 3000 CFU · m^{-3}.

the thermal inactivation performance for five kinds of bacteria. Basically, E. coli, L. monocytogenes, L. plantarum, S. Senftenberg and S. cerevisiae could not be thermal inactivated when the PV coverage was bigger than 0.4, 0.3, 0.6, 0.5 and 0.6, respectively. Different bacteria had different resistances to the thermal inactivation. Therefore, a balance between the thermal inactivation and the electrical performance should be considered. Bigger PV coverage can keep excellent electrical output while limits the thermal inactivation process of bacteria. Different bacteria presented different values of CADR under different PV coverages. In a similar way, for all bacteria, with the increase of the PV coverage, the CADR gradually decreased and approached to 0 when the PV coverage was bigger than certain value. By calculation, the total generated volume of fresh air decreased with the PV coverage quickly and approached to 0 under the PV coverage of 0.4 ~ 0.5. For example, for the PV coverage of 0.2, the total generated volume of fresh air for five kinds of

bacteria were 134.5, 92.4, 157.1, 137.9 and 155.3 m^3, respectively. Therefore, from the viewpoint of the system comprehensive performance, the electrical energy was the additional product and the low PV coverage was suggested.

5 Conclusions

A novel purified PV-Trombe wall for electricity, space heating, formaldehyde degradation and bacteria inactivation was proposed. The electrical performance, air thermal performance, formaldehyde degradation performance and the inactivation performance of five kinds of bacteria were investigated. The main conclusions were as follows:

(Ⅰ) When the PV coverage was 0, the average daily air thermal efficiency was 0.46, the formaldehyde single-pass ratio and the total generated volume of clean air were 0.35 and 93.4 m^3, respectively. At the same time, the investigative bacteria were all fully thermal inactivated for several hours in a day. The total generated volume of clean air were 188.3, 173.0, 201.4, 189.9 and 200.2 m^3 for E. coli, L. monocytogenes, L. plantarum, S. Senftenberg and S. cerevisiae, respectively.

(Ⅱ) The PV coverage only had a positive influence on the electrical performance and had negative effect on other performances such as thermal, formaldehyde degradation and bacteria inactivation performances. Considering the system comprehensive performance, the small PV coverage such as 0.2 or 0.3 was suggested.

(Ⅲ) The investigative bacteria had obvious thermal sensibility. Under fully same thermal conditions, the thermal sensitivity of five kinds bacteria follows the order of L. monocytogenes < E. coli < S. Senftenberg < L. plantarum < S. cerevisiae.

Acknowledgments

This work is supported by the Fundamental Research Funds for the Central Universities (WK2090000018) and the National Natural Science Foundation of China (51908527).

Conflict of interest

The authors declare no conflict of interest.

Author information

LI Niansi is currently a PhD student in the Department of Thermal Science and Energy Engineering under the supervision of Prof. Ji Jie at University of Science and Technology of China. Her research mainly focuses on solar energy utilization.

LIU Xiaoyong is currently a laboratory director at Inspection and Testing Center, Hefei Institute for Public Safety Research, Tsinghua University. His research mainly focuses on public safety.

YU Bendong is currently a post-doctor in the Department of Thermal Science and Energy Engineering at University of Science and Technology of China. Her research mainly focuses on solar energy utilization.

References

[1] Zhang T, Tan Y, Yang H, et al. The application of air layers in building envelopes: A review. Applied Energy, 2016, 165:707-734.

[2] Rabani M, Kalantar V, Dehghan A A, et al. Experimental study of the heating performance of a Trombe wall with a new design. Solar Energy, 2015,118:359-374.

[3] Zhou L, Huo J, Zhou T, et al. Investigation on the thermal performance of a composite Trombe wall under steady state condition. Energy and Buildings, 2020,214:109815.

[4] Ma Q, Fukuda H, Wei X, et al. Optimizing energy performance of a ventilated composite Trombe wall in an office building. Renewable Energy, 2019,134:1285-1294.

[5] Hong X, Leung MK, He W. Effective use of venetian blind in Trombe wall for solar space conditioning control. Applied Energy, 2019,250:452-460.

[6] Rabani M, Kalantar V, Dehghan AA, et al. Empirical investigation of the cooling performance of a new designed Trombe wall in combination with solar chimney and water spraying system. Energy and Buildings, 2015,102:45-57.

[7] Jie J, Hua Y, Gang P, et al. Study of PV-Trombe wall assisted with DC fan. Building and Environment, 2007,42:3529-3539.

[8] Jie J, Hua Y, Wei H, et al. Modeling of a novel Trombe wall with PV cells. Building and Environment, 2007,42:1544-1552.

[9] Lin Y, Ji J, Zhou F, et al. Experimental and numerical study on the performance of a built-middle PV Trombe wall system. Energy and Buildings, 2019,200:47-57.

[10] Xu L, Luo K, Ji J, et al. Study of a hybrid BIPV/T solar wall system. Energy, 2020,193:116578.

[11] Xu L, Ji J, Luo K, et al. Annual analysis of a multi-functional BIPV/T solar wall system in typical cities of China. Energy, 2020,197:117098.

[12] Wang D, Zhu B, He X, et al. Iron oxide nanowire-based filter for inactivation of airborne bacteria. Environmental Science: Nano, 2018,5:1096-1106.

[13] Lee Y H, Lee B-U. Inactivation of airborne E. coli and B. subtilis bioaerosols utilizing thermal energy. Journal of Microbiology and Biotechnology, 2006,16:1684-1689.

[14] Zhu X, Lv M, Yang X. Performance of sorption-based portable air cleaners in formaldehyde removal: Laboratory tests and field verification. Building and Environment, 2018,136:177-184.

[15] Yu B, Liu X, Li N, et al. The performance analysis of a purified PV/T-Trombe wall based on thermal catalytic oxidation process in winter. Energy Conversion and Management, 2020,203:112262.

[16] Yu B, Hou J, He W, et al. Study on a high-performance photocatalytic-Trombe wall system for space heating and air purification. Applied Energy, 2018,226:365-380.

[17] Sun Y, Zhang B, Zheng T, et al. Regeneration of activated carbon saturated with chloramphenicol by microwave and ultraviolet irradiation. Chemical Engineering Journal, 2017,320:264-270.

[18] Bai B, Qiao Q, Li J, et al. Progress in research on

catalysts for catalytic oxidation of formaldehyde. Chinese Journal of Catalysis, 2016,37:102-222.
[19] Yu B, He W, Li N, et al. Experimental and numerical performance analysis of a TC-Trombe wall. Applied Energy, 2017,206:70-82.
[20] Hwang G B, Jung J H, Jeong T G, et al. Effect of hybrid UV-thermal energy stimuli on inactivation of S. epidermidis and B. subtilis bacterial bioaerosols. Science of The Total Environment, 2010,408:5903-5909.
[21] Lee BU. Life comes from the air: A short review on bioaerosol control. Aerosol and Air Quality Research, 2011,11:921-927.
[22] McGuigan K, Joyce T M, Conroy RM, et al. Solar disinfection of drinking water contained in transparent plastic bottles: Characterizing the bacterial inactivation process. Journal of Applied Microbiology, 1998,84:1138-1148.
[23] Jin Y, Wang Y, Huang Q, et al. The performance and applicability study of a fixed photovoltaic-solar water disinfection system. Energy Conversion and Management, 2016,123:549-558.
[24] Ibrahim A, Othman M Y, Ruslan M H, et al. Recent advances in flat plate photovoltaic/thermal (PV/T) solar collectors. Renewable and Sustainable Energy Reviews, 2011,15:352-365.
[25] Yu B, He W, Li N, et al. Thermal catalytic oxidation performance study of SWTCO system for the degradation of indoor formaldehyde: Kinetics and feasibility analysis. Building and Environment, 2016,108:183-193.
[26] Guo C, Ji J, Sun W, et al. Numerical simulation and experimental validation of tri-functional photovoltaic/thermal solar collector. Energy, 2015,87:470-480.
[27] Duffie J A, Beckman W A. Solar engineering of thermal processes. Hoboken,NJ: Wiley, 1980.
[28] GreenM A, Dunlop E D, Levi D H, et al. Solar cell efficiency tables (version 54). Progress in Photovoltaics: Research and Applications, 2019,27:565-575.
[29] Xu Q, Zhang Y, Mo J, et al. Indoor formaldehyde removal by thermal catalyst: Kinetic characteristics, Key parameters, and temperature influence. Environmental Science & Technology, 2011,45:5754-5760.
[30] Fernández-Hernández F, Cejudo-López J M, Domínguez-Muñoz F, et al. A new desiccant channel to be integrated in building facades. Energy and Buildings, 2015, 86: 318-327.
[31] Yu B, Jiang Q, He W, et al. The performance analysis of a novel TC-Trombe wall system in heating seasons. Energy Conversion and Management, 2018, 164:242-261.
[32] Mastwijk H C, Timmermans R A H, Van Boekel M A J S. The Gauss-Eyring model: A new thermodynamic model for biochemical and microbial inactivation kinetics. Food Chemistry, 2017,237:331-341.
[33] Timmermans R, Mastwijk H, Groot M N, et al. Evaluation of the Gauss-Eyring model to predict thermal inactivation of micro-organisms at short holding times. International Journal of Food Microbiology, 2017,263:47-60.
[34] Zhao D, Ji J, Yu H, et al. Numerical and experimental study of a combined solar Chinese kang and solar air heating system based on Qinghai demonstration building. Energy and Buildings, 2017,143:61-70.
[35] Pei J, Han X, Lu Y. Performance and kinetics of catalytic oxidation of formaldehyde over copper manganese oxide catalyst. Building and Environment, 2015,84:134-141.

用于净化除菌的新型净化型光伏 Trombe 墙性能研究

李念思[1,2],刘小勇[2,3],余本东[1*]
1. 中国科学技术大学热科学和能源工程系,安徽合肥 230026;
2. 清华大学合肥公共安全研究院检验检测中心,安徽合肥 230601;
3. 灾害环境人员安全安徽省重点实验室,安徽合肥 230601
* 通讯作者. E-mail: bendong@mail.ustc.edu.cn

摘要: PV-Trombe 墙是一种太阳能利用系统,能实现室内采暖和产电双重功能,但其对太阳热的利用非常有限. 热催化氧化和热杀菌是两种先进的空气净化技术,利用太阳热能进行热脆化氧化和除菌杀毒具有巨大的应用潜力. 基于此,提出了一种新型的净化 PV-Trombe 墙,能实现产电、室内采暖、甲醛降解和除菌. 首先,建立了净化 PV-Trombe 墙的传热传质模型,并通过实验数据进行了验证. 其次,分析了光伏覆盖率为 0 时的综合性能. 最后,研究了光伏覆盖率对系统性能的影响. 结果表明:①PV 覆盖率为 0 时,平均日空气热效率为 0.46,甲醛单通率为 0.35;甲醛降解产生的洁净空气总量为 93.4 m^3;五种细菌被完全热灭活了几个小时. 大肠杆菌、单核增生杆菌、植物杆菌、森夫滕伯格菌和酿酒酵母失活产生的洁净空气总生成量分别为 188.3、173.0、201.4、189.9 和 200.2 m^3. ②光伏覆盖率对系统综合性能的影响不同. 就特定性能而言,光伏覆盖率仅对电性能有正向影响,对其他性能如热性能、甲醛降解性能和除菌性能有负面影响. 但考虑到系统的综合性能,建议电能为附加产品,光伏覆盖率较低. ③系统可为新冠肺炎疫情防控提供支持.

关键词: Trombe 墙;光伏;太阳能杀菌;太阳能热催化氧化;空间加热